Research Square

Preprints are preliminary reports that have not undergone peer review.
They should not be considered conclusive, used to inform clinical practice,
or referenced by the media as validated information.

Formation of Electrosprayed PVP-GTE Submicron Particles: Physicochemical Characteristics and Antioxidant Activities

Kamaruddin Kamaruddin

kamaruddin@unima.ac.id

Manado State University

Sri Hastuty

Universitas Pertamina

Khairurrijal Khairurrijal

Bandung Institute of Technology3Department of Physics

Research Article

Keywords: Electrospraying, Polyvinylpyrrolidone, Green Tea Extract, Encapsulation, Antioxidant Activity, Drug Delivery

Posted Date: June 16th, 2026

DOI: https://doi.org/10.21203/rs.3.rs-9905231/v1

License: This work is licensed under a Creative Commons Attribution 4.0 International License.
Read Full License

Additional Declarations: No competing interests reported.

Version of Record: A version of this preprint was published at Journal of Materials Science: Materials in Engineering on September 5th, 2026. See the published version at https://doi.org/10.1186/s40712-026-00589-5.

Formation of Electrosprayed PVP-GTE Submicron Particles: Physicochemical Characteristics and Antioxidant Activities

Kamaruddin Kamaruddin[1,*], Sri Hastuty[2] and Khairurrijal Khairurrijal[3,4,5,]

[1]Department of Physics, Faculty of Mathematics, Natural Sciences and Earth, Universitas Negeri Manado, Jl. Kampus Unima, Kabupaten Minahasa 95618, Indonesia
[2]Department of Mechanical Engineering, Universitas Pertamina, Jl. Teuku Nyak Arief, Simprug, Kebayoran Lama, Jakarta 12220, Indonesia
[3]Department of Physics, Faculty of Mathematics and Natural Sciences, Institut Teknologi Bandung, Jalan Ganesa 10, Bandung 40132, Indonesia
[4]Bioscience and Biotechnology Research Center, Institut Teknologi Bandung, Jalan Ganesa 10, Bandung 40132, Indonesia
[5]Center for Green and Sustainable Materials, Institut Teknologi Sumatera, Jalan Terusan Ryacudu, Lampung, Selatan, 35365, Indonesia

[*]*Email: kamaruddin@unima.ac.id*

ABSTRACT

This research is focused on the optimation of green tea extract-loaded polyvinylpyrrolidone (PVP) submicron particles by electrospraying for enhanced delivery of antioxidants. The novelty lies in the explanation of the critical connection between process parameters, drug loading, and biological activity. A precursor solution of GTE and PVP in ethanol (13 wt.%) was electrosprayed at a fixed voltage (15 kV) and distance (15 cm), and the flow rate varied (1, 3, and 5 μL/min) as an important parameter. Spherical morphologies were examined using scanning electron microscopy (SEM), with the average diameter of particles increasing from 391 nm to 713 nm with increasing flow rate. FTIR spectroscopy employing Fourier transform infrared verified effective encapsulation of the GTE in the PVP matrix via hydrogen bonding. Differential scanning calorimetry (DSC) and X-ray diffraction (XRD) analysis indicated that the encapsulated GTE existed in an amorphous form, a desired state for enhanced bioavailability. More importantly, diphenylpicrylhydrazyl (DPPH) assay demonstrated pronounced antioxidant activity in the composite particles to be significantly enhanced relative to free GTE (IC_{50} values of ~22 μg/mL vs. 47 μg/mL). Compared to typical emphasis on nano-size for rapid release, bigger particles (separated at higher flow rates) contained superior antioxidant activity with higher GTE loading content (~47%), overshadowing kinetic advantage of smaller particles. The above findings emphasize that optimization of encapsulation efficiency can be more crucial than mere size decrease. Thus, electrosprayed PVP-GTE particles reveal a highly promising platform for creating efficient natural antioxidant delivery systems.

Keywords: Electrospraying, Polyvinylpyrrolidone, Green Tea Extract, Encapsulation, Antioxidant Activity, Drug Delivery

1. Introduction

The development of drug delivery systems based on natural bioactive compounds has gained increasing attention in recent years, in line with the rising demand for functional food and pharmaceutical products with higher therapeutic effectiveness. In drug delivery systems, nano-structured particles composed of biodegradable polymers provide promising assurance in meeting specific criteria, such as transformability, stability during aerosolization, biocompatibility, target site specificity, controlled drug release, and degradation within an acceptable timeframe [1]. Moreover, polymers offer advantages in controlling drug release rates, enhancing solubility, breaking down into biologically metabolizable molecules, masking unpleasant tastes, improving drug stability, and modifying release characteristics [2,3]. Based on these explanations, specific studies are required to produce nano-sized and nano-structured morphologies, such as nanoparticles, including drug or active substance loading, in order to determine their morphological structure and pharmacological characteristics. Between the various encapsulation techniques, electrospray has been a potential method for producing controlled morphology and narrow size distribution. The method is suitable for the encapsulation of bioactive compounds within a polymer matrix for enhancing their stability, solubility, and bioavailability.

One of the most rapidly developing and widely used methods for the production of micro to nano-scale particles is the electrospray method. Electrospraying is a variation of the electrospinning method and is more commonly known as electrohydrodynamic atomization (EHDA) or electrohydrodynamic (EHD) spraying. This engineering technique utilizes electrostatic forces on the surface of a polymer solution due to a very high potential difference, resulting in the formation of particles or fibers [4–6]. The method has been widely used due to its advantages in controlling morphology, particle size, cost-effectiveness, and ease of implementation [5–7]. There are several parameters on this method which are directly correlated to morphology and size controlled. The solution-related properties (additives, solvent mixture, and

concentration) and the process-related parameters (collector geometry, environmental conditions, needle-to-collector distance, flow rate, and applied voltage) are these parameters [8,9]. A research conducted by [5] described a strong relationship between the phase of particle formation towards fibers or vice versa, with viscosity, surface tension, and flow rate being crucial in morphological control and size during the process. Therefore, electrospray process can be said to be an excellent technique for preparing polymers-loaded drug particles [10]. Electrospray can produce diverse morphologies such as fibers, rods, or spheres depending on processing conditions [11,12]. Spherical or hemispherical particles are ideal due to their uniform surface area and superior functional performance, yet they are difficult to obtain consistently due to the sensitivity of process parameters [13].

Nevertheless, consistently reproducible methods for generating bioactive polymer-based molecules for biomedical applications still face many challenges [14]. A deeper understanding of electrospraying for encapsulation has been reported by [15] which is crucial, as this method may improve bioavailability, biological activity, and overall characteristics of various food products. Furthermore, developed formulations are directed toward targeted drug delivery systems with controlled release capabilities [16]. Various natural bioactive compounds, such as polyphenols, are known to possess therapeutic properties and are highly potential candidates for further formulation, such as extracts from functional food plants. Green tea is one of the most popular beverages consumed for health benefits. Its chemical composition is similar to that of fresh leaves, particularly due to its polyphenol content [12,17,18]. Moreover, polyphenols in green tea exhibit strong antioxidant activity [17,19–21]. Polyphenolic compounds have been proven to possess pharmacological actions in prevention, treatment, and high antioxidant activity [18,22–24].

Therefore, in this study, we aim to comprehensively report our research on producing submicron composite particles with the potential to encapsulate bioactive compounds from green tea extract using Polyvinylpyrrolidone (PVP) as the polymer matrix. PVP was selected as the matrix because it is widely used, non-toxic, water-soluble, biocompatible, and recognized as safe for healthcare applications by the U.S. Food and Drug Administration (FDA). Our previous research successfully formulated PVP-GTE using the electrospray technique [25]. Subsequently, we optimized the process by considering solution parameters and obtained pure spherical submicron-sized composite particles [26]. While electrospraying of PVP-GTE has been reported [25,26], a comprehensive study correlating process parameters (e.g., flow rate) with critical quality attributes like drug loading, release profile, and resultant pharmacological efficacy is still lacking.

Therefore, this study is extended to thoroughly investigate the effect of a key process parameter (flow rate) on the encapsulation of green tea extract using electrospraying. The goal is to produce superior particle formation and directly correlate it with pharmacological assessments, such as antioxidant activity testing. In this study, the electrospray process is further analyzed to examine the effects of process parameters (flow rate) on morphology and size, molecular interactions, thermal stability, crystallinity, and pharmacological properties. The PVP-GTE composite particles were characterized morphologically using scanning electron microscopy (SEM), molecular interactions using Fourier transform infrared spectroscopy (FTIR), thermal properties using differential scanning calorimetry (DSC), crystallinity using x-ray diffraction (XRD), and pharmacological properties. Pharmacological characterizations included antioxidant activity testing.

2. Materials and Methods

2.1. Materials and Sample Preparation

Green tea leaves were purchased from a local market in Bandung, Indonesia. Polyvinylpyrrolidone (PVP, MW 40,000 $g \cdot mol^{-1}$), 1,1-diphenyl-2-picrylhydrazyl (DPPH), and analytical-grade ethanol were obtained from Sigma-Aldrich (Indonesia). Ethanol of technical grade with 96% purity, along with deionized water, was obtained from Bratachem, Indonesia. Green tea extract (GTE) was prepared by maceration to obtain powdered extract at the Natural Product Laboratory, Bioscience and Biotechnology Research Center (BBRC), Bandung Institute of Technology (ITB). PVP was dissolved in ethanol diluted with deionized water (7:3 w/w) to obtain a 15 wt.% PVP solution. Polymer concentration and solvent composition were selected from previous work [5] that was proven to be optimal for particle formation. GTE was dissolved in 10 wt.% ethanol [26]. PVP and GTE solutions were shaken for approximately one hour before mixing. The solutions were blended at different asymmetric ratios and stirred for two hours at room temperature using a magnetic stirrer. At 6:4 PVP-to-GTE ratio, the most uniform precursor solution was obtained, which is equivalent to a 13 wt.% PVP-GTE solution containing 0.9 g PVP and 0.4 g GTE. Solution properties were determined using a Fenske-Ostwald viscometer (Fisher), a du Noüy tensiometer (Fisher), and a conductometer (Mettler Toledo). The measured values were: viscosity = 7.368 cP, surface tension = 32.1 dyne/cm, and conductivity = 2.36 µS/cm [26]. The PVP solution appeared transparent white, while the GTE solution was dark brown; the mixed PVP-GTE solution was also dark brown. The precursor solution was subsequently processed using the electrospraying apparatus.

2.2. Electrospraying Process

The electrospraying apparatus is schematically shown in **Figure 1**. A Terumo 1 mL syringe was loaded with the PVP-GTE precursor solution and subjected to a high voltage of 15 kV for initiating electrospraying. The grounded electrode was an aluminum foil-covered collector plate, positioned 15 cm away from the needle of the syringe (27 gauge = 0.36 mm). Spraying was done within an acrylic chamber at room temperature and humidity regulated at 60–70%. Flow rate was regulated at 1, 3, and 5 µL/min, designated as PG1, PG3, and PG5, respectively. The syringe pump was regulated by a PC through dedicated software. Real-time spray modes were visualized using a high-speed digital camera (Panasonic, M2050).

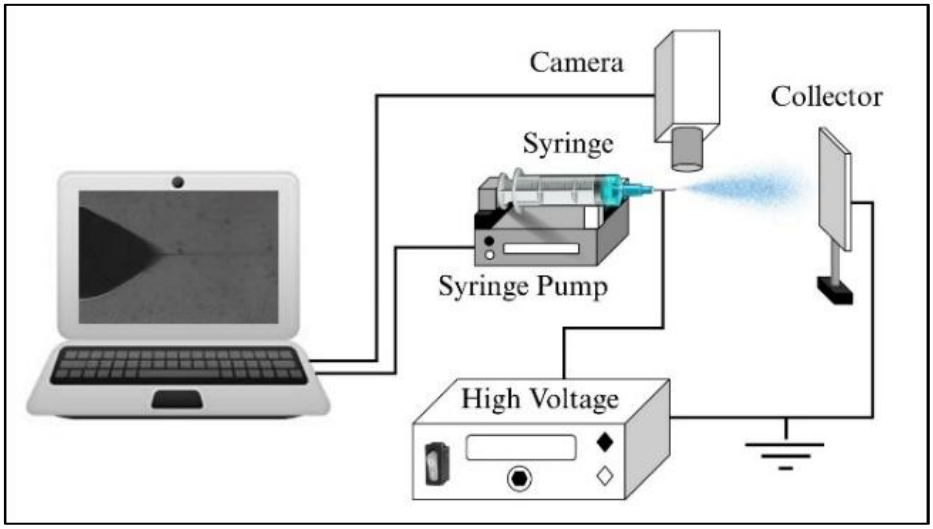


Figure 1. Schematic diagram of the electrospraying apparatus used in this study.

2.3. Morphology and Size

The morphology of electrosprayed particles was examined with a scanning electron microscope (SEM, Hitachi SU3500) at 5 kV and 10,000X magnification. The mean diameter of the particles was determined using 300 measurements with Image-MIF v3.0 software, and the size distribution was analyzed by Origin 9.0.

2.4. Fourier Transform Infra-Red Spectroscopy

Fourier transform infrared (FTIR) spectroscopy (Bruker, Alpha 1-176-396) was used to determine the functional groups present and to evaluate the intermolecular interactions occurring between PVP and GTE in the composite particles. The spectra were recorded in the range of wavenumbers of 500–4000 cm^{-1}.

2.5. XRD Characterization

Crystalline structure of samples was analyzed using x-ray diffraction (XRD) at 2θ angles between 10° and 90°. The analysis was performed on a Rigaku diffractometer at the Hydrogeology Laboratory, Mining Engineering Department, ITB, with 40 kV and 30 mA conditions and a Cu anode filter. The samples examined include PVP powder, electrosprayed PVP, GTE powder, and PVP-GTE composite particles with different flow rates.

2.6. DSC Characterization

Thermal characteristics were examined using differential scanning calorimetry (DSC 4000, Perkin Elmer) in Microstructure Laboratory, Department of Physics, Universitas Negeri Makassar. The heating rate was 10 °C/min. Sample of PVP powder, electrosprayed PVP, GTE powder, and PVP-GTE composites of various flow rates were used for testing.

2.7. The GTE Content Assay and the Antioxidant Activity

The GTE content in PVP-GTE composite particles was determined using UV–Visible spectrophotometry (Beckman DU-7500i). A calibration curve was prepared by dissolving GTE in analytical-grade ethanol at concentrations of 15, 20, 25, 30, 35, 40, and 45 $\mu g \cdot mL^{-1}$, and the absorbance was measured at 274 nm. The calibration equation ($y = mx + c$) was then applied to calculate the GTE concentration in the samples. For analysis, the composite particles were suspended at a concentration of 100 µg particles·mL^{-1}, and the dissolved GTE was measured at λ = 274 nm. The obtained GTE

concentrations (μg·mL⁻¹) were substituted into the calibration equation and subsequently converted into loading content (LC, % w/w) relative to the particle mass (100 μg·mL⁻¹). Each measurement was performed in triplicate to ensure data reliability.

Antioxidant activity was evaluated using the DPPH assay [27–29]. Activity was calculated using Equation (1):

$$\%AA = \left[\frac{A_{control} - A_{sample}}{A_{control}}\right] x\ 100\% \qquad (1)$$

where $A_{control}$ is the absorbance of a 25 ppm DPPH solution without composites, and A_{sample} is the absorbance of a 50 ppm DPPH solution mixed with 50 ppm PVP-GTE particles (1:1 v/v with ethanol) after incubation for 30 min in the dark. Absorbance spectra were recorded at 517 nm, corresponding to the DPPH absorption maximum [27,30].

3. Results and Discussion

3.1. Morphology, Size, and Spraying Modes

Polyvinylpyrrolidone (PVP) loaded with green tea extract (GTE) was successfully electrosprayed under different flow rate conditions, confirming the feasibility of this technique for producing submicron-sized particles. These findings highlight electrospraying as a promising method for formulating pharmaceutical materials intended for drug delivery applications. The morphological features of the PVP-GTE composite particles were characterized using scanning electron microscopy (SEM) at 10,000× magnification. Representative SEM micrographs, particle size distributions, and spray modes observed during electrospraying are presented in **Figure 2**.

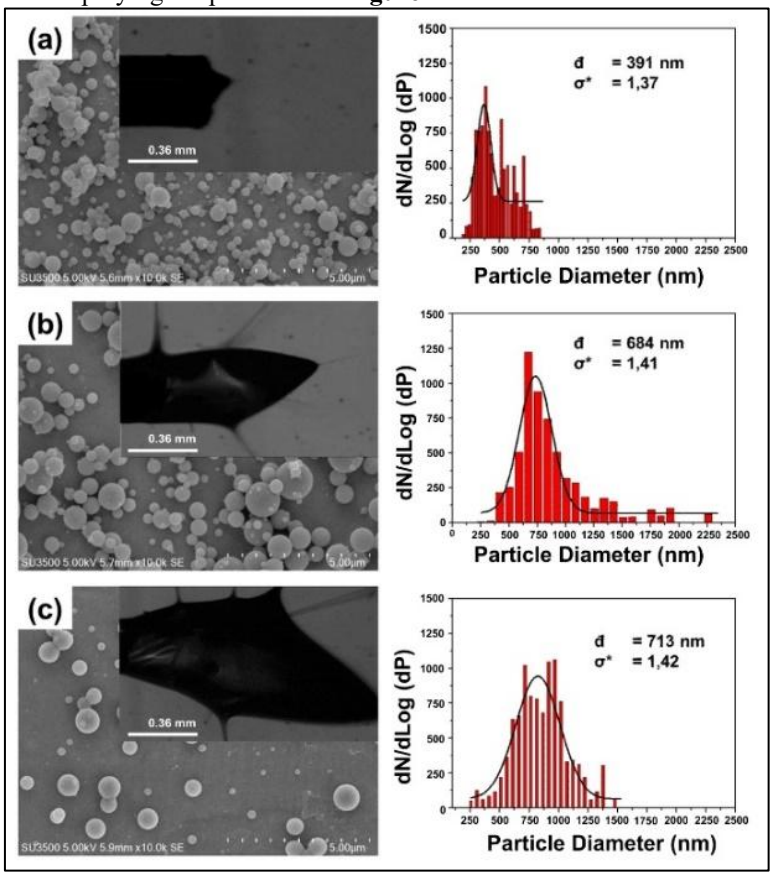


Figure 2. The SEM images, Spraying Modes (Inset pictures), and particles diameter distribution of PVP-GTE composite particles obtained under three different flow rates (a) 1 μL/min (PG1), (b) 3 μL/min (PG3), and (c) 5 μL/min (PG5).

Figure 2. displays SEM images showing the morphology of PVP-GTE particles with varying flow rates, all of which are spherical. These results align with and improve upon our previous study, which also used the same PVP-GTE material but produced bead-fibers [25] and particles with different parameters [26]. In contrast, [31] reported fiber formation under similar conditions which produced fibers. In principle, this method can produce fibers, beads, fiber beads, and pure particles depending on the applied parameters [5]. Therefore, this method holds great promise for application in the pharmaceutical industry. Particle morphology influences many properties, including solubility, bioavailability, dissolution rate, flowability, and compliance, thus impacting the overall efficacy of pharmaceutical formulations [32,33]. According to [34], pharmaceutical particles originating from solid suspensions can be viewed as systems in which the

dispersed phase consists of smaller solid entities embedded within a continuous phase. In the case of PVP-GTE particles, PVP serves as the continuous polymeric matrix, while GTE molecules act as the dispersed phase. The amount of GTE that can be successfully encapsulated is directly related to the capacity of the PVP matrix to accommodate and stabilize the bioactive compounds. There are two possible formations to encapsulate the GTE as a bioactive compound, as shown in **Figure 3(b).**

Meanwhile, the results of the PVP-GTE diameter measurements resulting from variations in flow rate are shown in the bar chart in **Figure 2**. The calculated particle diameters of PG1, PG3, and PG5 are in the range of 169-831, 195-2190, and 216-1429 nm, respectively, with average values of 391, 684, and 713 nm. The geometric standard deviation calculations of PG1, PG3, and PG5 are 1.37, 1.41, and 1.42, respectively. Based on the calculated geometric standard deviation, the particles showed a wide and polydisperse size distribution. Based on [35], uniformity was classified when the geometric standard deviation was ≤1.22. The result was found that the average diameter of particles increases with the increase of flow rates, which is consistent with previous work [5,36]. Moreover, flow rate is the most important operating parameter where particle size increases with flow rate [37,38]. This broad distribution is attributed to the instability of the electrospray jet, which transitioned from an oscillating jet mode at 1 µL/min to a multi-jet mode at higher flow rates (3 and 5 µL/min), as visualized in the inset of **Figure 2.** This jet instability leads to the production of particles with a wide size distribution, a phenomenon that has been previously reported [39]. The spray mode mechanism can be seen in **Figure 3**.

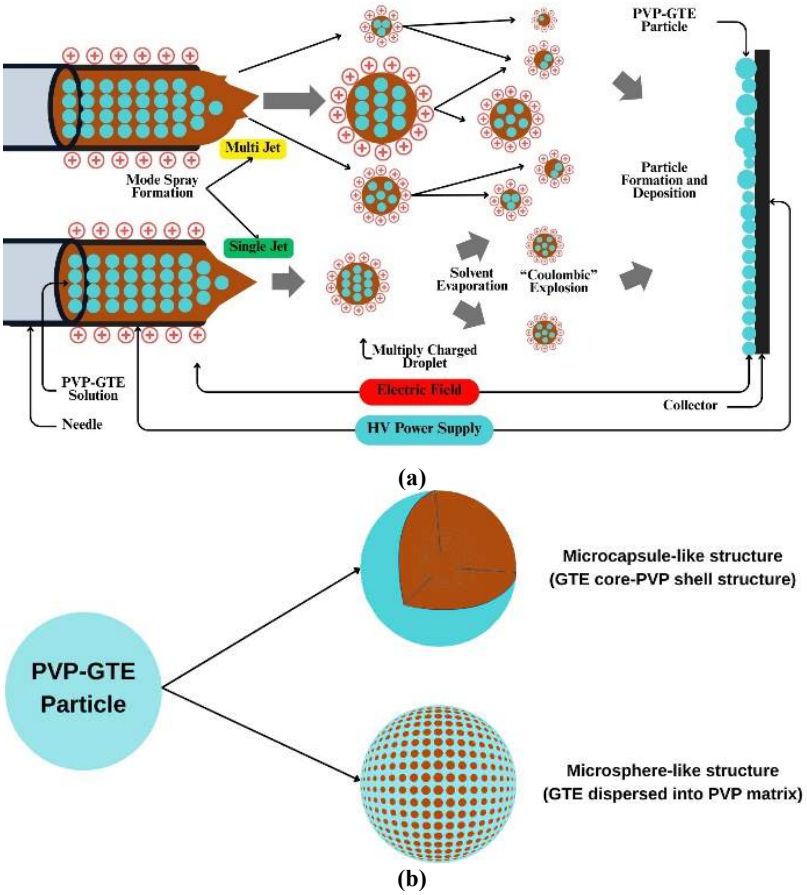


Figure 3. The illustration of (a) mechanism of particle formation based on spraying modes during electrospraying process and (b) possible PVP-based particle formation [11]

Figure 3(a). illustrates the particle formation mechanism during the electrospraying process. Applying high voltage to a syringe needle coupled to a grounded collector generates a strong electric field between the two. This electric field generates a Coulomb force that triggers the formation of a jet and spray from the precursor solution. The flow of the precursor solution is continuously controlled by a syringe pump, ensuring a stable jet and spray formation process. The resulting charged droplets move toward the collector and undergo rapid shrinkage due to solvent evaporation. Furthermore, the droplets can undergo a Coulombic explosion, producing a large number of smaller daughter droplets. This process is similar to the research reported by [40]. However, highly monodisperse particles such as microparticles and nanoparticles can be produced by controlling the electrospray parameters to obtain a Taylor cone-jet spray mode [38,41]. As with the observed results as shown in **Figure 2**, the inserted image shows the variation of flow rate which is

one of the process parameters in the electrospray method resulting in various spray modes. The mode spray of PG1 was oscillating jet while PG3 and PG5 were multi-jet [42]. Thus, the jet instability of the PVP-GTE electrospraying process at these parameters results in submicron particles and non-uniform size distribution.

On the other hand, the particle size measured for PVP-GTE composites was analyzed in relation to the theoretical model. This model suggests that the diameter of electrosprayed particles depends on both the flow rate and the conductivity of the solution, described by [36,43]:

$$D_{drop} = G(\kappa)\left(\kappa\varepsilon_0 \frac{Q}{K}\right)^{1/3} \qquad (1)$$

$$D_{comp} = G(\kappa)\left(\phi\kappa\varepsilon_0 \frac{Q}{K}\right)^{1/3} \qquad (2)$$

where D_{drop} refers to the predicted droplet size, D_{comp} corresponds to the composite particle diameter, κ is the dielectric constant, Q is the flow rate, ϕ is the volume fraction of the composites, and ε_0 corresponds to the permittivity of free space. Here, K stands for electrical conductivity, and $G(\kappa)$ is a dimensionless function defined as follows:

$$G(\kappa) = -10.9\kappa^{-6/5} + 4.08\kappa^{-1/3}. \qquad (3)$$

Figure 4. illustrates the estimated droplet diameters predicted by Eq. (1) and (2). The triangular and square markers represent data derived from polymer–pigment–nanoparticle composites [36] and pure polymer systems [43], respectively. In contrast, the circular and star symbols correspond to data from green tea extract composites, reported previously [26] and and obtained in the present study, plotted as the logarithm of diameter (D) versus the logarithm of Q/K.

As illustrated in Figure 4, the experimental findings were in reasonable agreement with the theoretical model. In this study, the experimental data were fitted to the model by varying the flow rate in the range of 10^4 to 10^5, representing roughly one order of magnitude. Consequently, the mean diameter of the electrosprayed particles could be linked to the predictive equations, indicating that particle size is tunable through adjustments in flow rate.

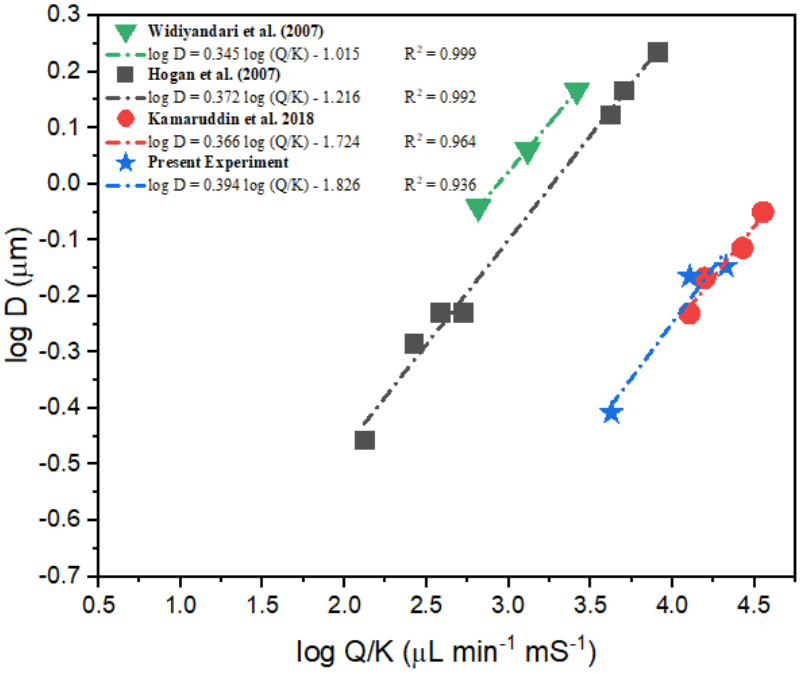


Figure 4. Experimental determined and theoretically initial droplet as predicted sizes of particle diameters during the electrospraying

3.2. Fourier Transform Infra-Red (FTIR) Spectra

Figure 5. shows the FTIR spectra of GTE, PVP, and PVP-GTE composite particles. In the FTIR spectrum of PVP (**Figure 5(a)**), the peak at 3417 cm^{-1} indicates O-H stretching of the hydroxyl group [25,44]. The peaks at 2954 and 1648 cm^{-1} proved the existence of asymmetric stretching of CH_2 and stretching of C-O, respectively [25,39]. The CH_2 wagging was observed at 1290 cm^{-1}, respectively [25,39]. Meanwhile, the GTE spectrum is given in **Figure 5.**(e), the broad peak at

3331 cm^{-1} represents the presence of O-H stretching of the hydroxyl group [25,45]. The peak of 2924 cm^{-1} was identified as asymmetric C-H alkanes stretch [25,45]. The group of C=C stretch in the aromatic ring and C=O stretch in polyphenols were characterized at 1689 and 1604 cm^{-1} in polyphenol, respectively [25,45]. The peak at 1335 cm^{-1} indicates C-O stretching in amino acid [25,45]. Therefore, these findings revealed that the GTE was rich in polyphenols similarly with our previous work.

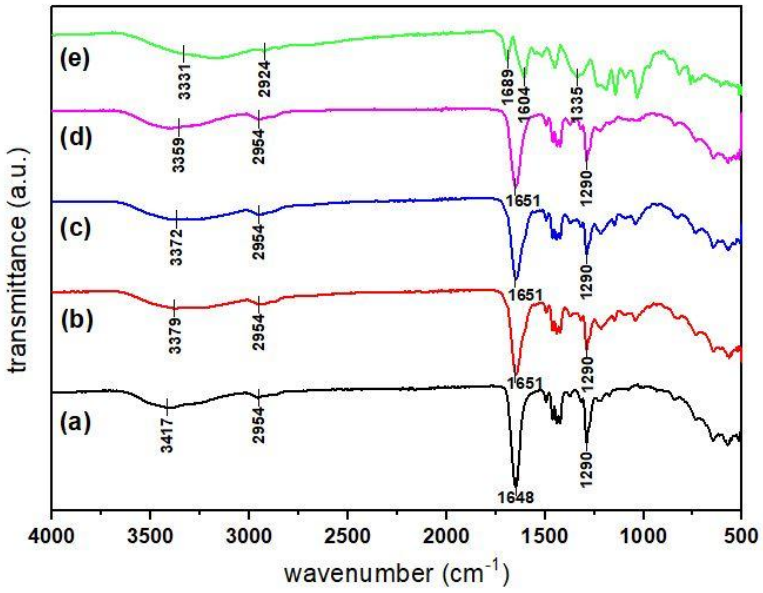


Figure 5. The FTIR Spectra of (a) PVP, (b) PG1, (c) PG3, (d) PG5, and (e) GTE

The FTIR spectra of PVP-GTE in **Figure 5.** (b), (c), and (d) as PG1, PG3, and PG5 show specific peaks at 3379, 3372, and 3359 cm^{-1}, respectively. The peaks at 2954, 1651, and 1290 cm^{-1} appeared not shifted. This characteristic presents that each peak of PVP-GTE composite stands between the peaks of PVP and GTE at broadband 3550-3200 cm^{-1} which are assigned as O-H stretching [44]. It suggested that the O-H stretching peak of the PVP-GTE composite submicron particles shifted to a higher wavenumber with increasing its flow rate as electrospraying parameter process. Therefore, the shifting peaks of PVP-GTE composite particles as PG1, PG3, and PG5 had intermolecular interactions between PVP and GTE via hydrogen bonds as OH groups of GTE [27,39].
Furthermore, the peak PVP-GTE composite particle at that band's shifts toward from the higher wavenumber as lower particle diameter to the lower wavenumber as the higher particle diameter of PVP-GTE composite particles. This result also shows the relationship of molecular interaction in PVP-GTE as the amount of GTE encapsulation. Similar results by composing the natural extract with polymer also shown the shifting the higher wavenumber to lower wavenumber as the presence of bioactive compound on polymer [27,39]. This is because adjusting the flow rates affects the amount of GTE encapsulated within the PVP-GTE composite particles. Moreover, a higher flow rate resulted in larger particle diameters and a higher GTE content. Thus, from the FTIR characteristics analyzed in this study, it can be concluded that GTE has been successfully encapsulating into PVP which is formulated in the form of PVP-GTE composite particles.

3.3. DSC Characterization

The results of thermal characterization using differential scanning calorimetry (DSC) are shown in **Figure 6**. The thermograms of all samples show endothermic curves. **Figure 6(a)** shows that the PVP powder curve exhibits a change in glass temperature (T_g) at 113,72 ^{0}C and PVP electrospray shows a melting temperature (T_m) at 128,20 ^{0}C. The DSC curve of GTE shows an endothermic response at 132,73 ^{0}C which indicates its melting temperature (T_m). Meanwhile, there was a change in the melting temperature (Tm) in samples PG1, PG3, and PG5, respectively, namely 113.14 ^{0}C, 124.89 ^{0}C, and 127.94 ^{0}C. This shows that the greater the flow rate of the electrospray solution has produced the larger the PVP-GTE composite particle size and caused the greater the increase in temperature. The relationship between particle diameter and thermal transition temperatures is consistent with the results that have been reported previously [40,46]. Another result obtained is the change in enthalpy (H) values in samples PG1, PG3, and PG5 which were -327.929, -300.125, and -274.79 J/g, respectively. These results indicate that the larger the diameter of the composite particles, the smaller the enthalpy change that occurs.

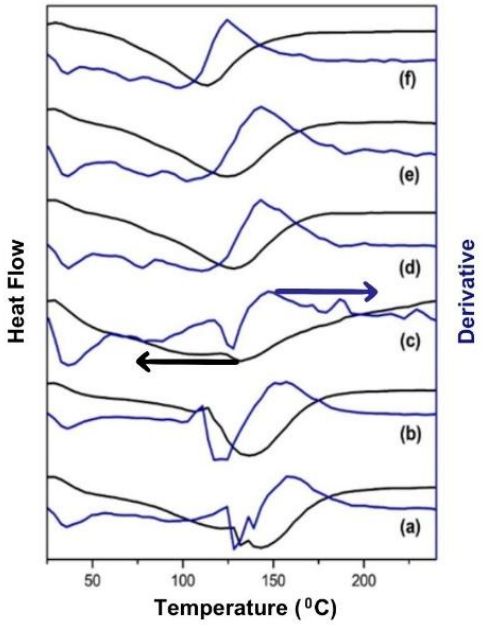


Figure 6. DSC thermograms (a) PVP powder, (b) PVP electrospray, (c) GTE, (d) PG1, (e) PG3, dan (f) PG5

3.4. XRD Characterization

The results of the phase structure characterization using x-ray diffraction (XRD) can be seen in **Figure 7**.

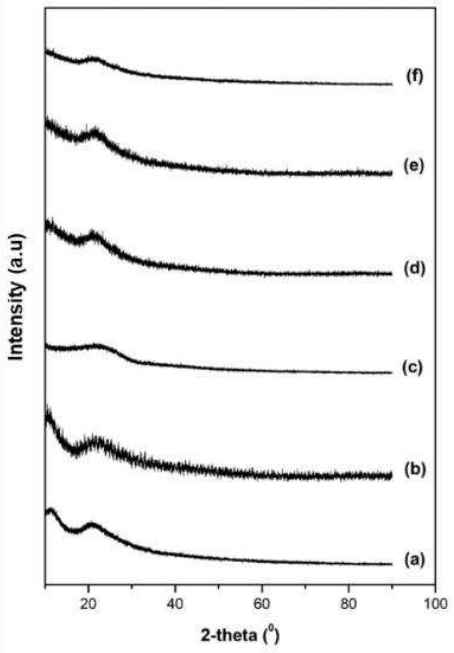


Figure 7. XRD pattern (a) PVP powder, (b) PVP electrospray, (c) GTE, (d) PG1, (e) PG3, dan (f) PG5

Figure 7. shows that the diffraction patterns of all characterized samples indicate an amorphous form. This is because there are no specific peaks for each sample, indicating a crystalline structure. Powdered PVP and electrosprayed PVP exhibit broad spectra with one valley and two shoulders between the 2-theta angles of 11.52° and 20.81°. A broad peak in GTE is observed at the 2-theta angle of 22.74°.

PVP-GTE composite particles with varying flow rates of PG1, PG3, and PG5 did not exhibit significant changes. However, the diffraction patterns generally indicate that GTE has been successfully loaded and formulated into PVP-GTE composite particles with an amorphous structure. An amorphous structure is a criterion in drug delivery systems due to its superior interaction capabilities compared to crystalline forms.

3.5. The GTE Content Assay and Antioxidant Activity

The relationship between particle size, the encapsulated bioactive content (loading content), and antioxidant activity is a crucial aspect in understanding the effectiveness of PVP-GTE particle formulations [16,47]. In general, particle size directly influences the encapsulation capacity and the release mechanism of bioactive compounds [39]. Smaller particles typically possess a larger specific surface area, that has thinner encapsulation make it to more vulnerable and then facilitates a faster release of active compounds. However, their internal volume is relatively limited, resulting in a lower loading content. Conversely, larger particles have greater internal capacity, allowing them to encapsulate more GTE molecules, although their release rate tends to be slower [36,43].

As highlighted by [11], PVP prevents the recrystallization of incorporated actives and enhances their solubility, thereby increasing the effective loading content. This explains the experimental observation that larger PVP-GTE particles (PG3, PG5) exhibit higher GTE loading content than smaller particles (PG1). The greater internal volume of larger particles allows more GTE molecules to be entrapped and stabilized by intermolecular interactions with PVP, leading to stronger antioxidant activity. Hence, the loading capacity is not only a function of particle diameter but also a manifestation of PVP's role as a stabilizing and solubilizing carrier, ensuring that higher GTE content can be retained within the particle structure

The GTE content in the PVP-GTE composite particles was measured using a UV-Vis spectrophotometer by generating a calibration curve of GTE. The antioxidant activity test using the DPPH method, as the IC_{50} values also measured. The GTE content and the IC_{50} values were shown in **Figure 8**.

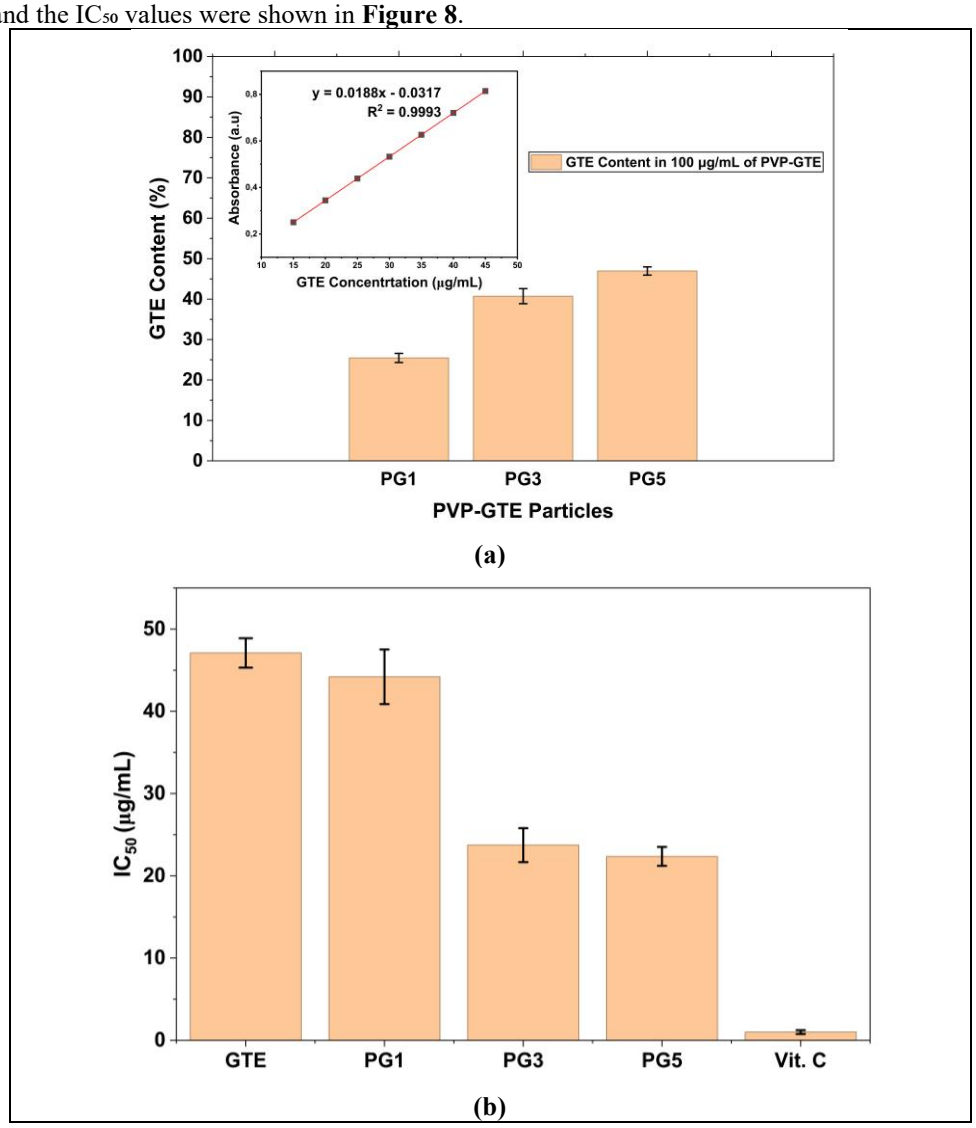


Figure 8. (a) The GTE content in on PVP-GTE Particles and (b) the IC_{50} values

As shown in the **Figure 8.(a)**, The quantity of GTE that was loaded on PG1, PG3, and PG5 was 25.45 ± 1.12, 40.72 ± 1.86, and 46.94 ± 1.02 µg/ml, respectively. In this study, the GTE content analysis showed an increase in loading content

with increasing particle diameter from PG1 to PG5. This phenomenon can be theoretically explained by the fact that particle volume increases proportionally with r^3, while surface area increases only with r^2. Thus, larger particles provide greater internal capacity for bioactive encapsulation [16]. Therefore, although smaller particles (PG1) may release GTE more rapidly, their lower GTE content results in weaker antioxidant activity compared to larger particles (PG3 and PG5) with higher GTE loading. This phenomenon is in line with the encapsulation model in the electrospray system [16,36,43].
The antioxidant activity test using the DPPH method further confirmed these findings, as the IC_{50} values decreased significantly as shown in **Figure 8.(b).** A decrease in IC_{50} value indicates an increase in the potential or activity of an antioxidant compound to inhibit 50% of DPPH free radicals. The lower the IC_{50} value, the lower the concentration required to achieve 50% inhibition, thereby indicating that the compound possesses stronger antioxidant activity. Thus, the higher the GTE content encapsulated in PVP, the stronger the antioxidant activity produced, because the number of polyphenol compounds is greater, protected by the polymer matrix, and able to interact more effectively with free radicals.
These findings indicate that the dominant factor in enhancing antioxidant activity is not solely particle size, but primarily the amount of GTE successfully encapsulated within the PVP matrix [39,47]. Hence, higher loading content in larger particles leads to stronger antioxidant activity compared to smaller particles, despite the theoretical advantage of faster release in the latter.
The Relationship between Particle Size, the loading content, and antioxidant activity was shown in **Table 1**.

Table 1. The Relationship between Particle Size, the loading content, and antioxidant activity

Samples	Average Particles Diameter (nm)	Loading Content (%)	IC_{50} (μg/mL)
GTE	-	-	47.10 ± 1.79
PG1	391	25.45 ± 1.12	44.20 ± 3.32
PG3	684	40.72 ± 1.86	23.73 ± 2.06
PG5	713	46.94 ± 1.02	22.36 ± 1.15
Vit. C	-	-	1.00±0.23

The relationship between particle diameter, loading content, and antioxidant activity can be more comprehensively understood by correlating the results of FTIR, DSC, and XRD characterization. First, FTIR analysis revealed a shift in the absorption band within the range of 3200–3400 cm^{-1}, indicating the formation of hydrogen bonds between the –OH groups of GTE polyphenols and the carbonyl groups of PVP [27,39]. This shift was more pronounced in samples with larger particle diameters (PG3, PG5), suggesting that a higher amount of encapsulated GTE leads to stronger intermolecular interactions [44]. Such interactions play a critical role in maintaining the stability of polyphenol molecules and preventing oxidative degradation, thereby supporting enhanced antioxidant activity.
Second, DSC results showed shifts and changes in the intensity of endothermic peaks in PG1, PG3, and PG5 compared to pure PVP and GTE. The decrease in enthalpy and the shifts in glass transition temperature (Tg) and melting temperature (Tm) indicated that GTE was dispersed within the PVP matrix, particularly in larger particles [46]. This provides further evidence that loading content increases with particle size, as more GTE is associated with PVP in the form of a homogeneous mixture [16].
Third, XRD patterns demonstrated an amorphous structure in PVP-GTE particles compared to the semi-crystalline peaks observed in pure GTE. The disappearance of crystalline peaks of GTE in PVP-GTE particles indicated that GTE molecules were amorphously distributed within the PVP matrix [27,39]. This amorphous structure is highly significant in drug delivery systems, as it enhances the solubility and bioavailability of active compounds [14], thereby directly contributing to the increased antioxidant activity observed in PG3 and PG5 .
Overall, the FTIR, DSC, and XRD data support the finding that larger particle diameters correspond to higher GTE loading content within the PVP matrix. This increase is evidenced by stronger molecular interactions (FTIR), altered thermal stability (DSC), and the formation of an amorphous phase (XRD). These results are consistent with the DPPH assay, which showed that higher loading content resulted in stronger antioxidant activity (lower IC_{50}) [16,47]. Therefore, the key determinant of enhanced antioxidant activity in this study is the degree of GTE encapsulation and its molecular interactions within PVP, which play a more dominant role than particle size alone.

4. Conclusion

This study successfully validates that the electrospraying technique is effective for fabricating GTE-loaded PVP composite particles. Most importantly, we established that the larger particles, achieved at higher flow rates, possess superior GTE loading content and consequently, significantly enhanced antioxidant activity compared to both smaller particles and pure GTE. SEM observations showed that PVP–GTE composites formed smooth, spherical particles ranging in size from microns to nanometers. The increase of flow rates shows the increased the diameter of particles. From the FTIR characterization, it was confirmed that GTE was successfully entrapped within the PVP structure through hydrogen

bonding, representing the molecular interactions between GTE and PVP in the PVP–GTE composites. Also, DSC and XRD characterization validated that the GTE was loaded into an amorphous phase within the PVP matrix, as evidenced by endothermic events. Antioxidant assays demonstrated that GTE retained its activity after the encapsulation process. The composite of PVP-GTE particles presented significantly higher antioxidant activity compared to pure GTE. This discovery has overturned the traditional hypothesis that only nanoparticle size is the most important feature of delivery systems by pointing out that encapsulation efficiency and payload capacity could be key factors of biological activity for certain applications. The upcoming study will work on how to optimize the formulation to get a size distribution with the least error without affecting the content carried and at the same time, the release profile and in-vivo models' efficacy will be assessed.

Conflict of interest

The authors declare that they have no competing interests or personal relationships that could have influenced the work reported in this paper.

Acknowledgements

K. Kamaruddin wishes to acknowledge the Endowment Fund for Education (LPDP) of the Republic of Indonesia for supporting the first author's Master's study at the Bandung Institute of Technology (ITB), conducted under the supervision of Kharurrijal and Muhammad Miftahul Munir. The completion of this article was further supported by the Inclusive Campus Program, Directorate of Talent Development, Ministry of Higher Education, Science, and Technology of the Republic of Indonesia.

REFERENCES

[1] Tiwari G, Tiwari R, Bannerjee S, Bhati L, Pandey S, Pandey P, Sriwastawa B. Drug delivery systems: An updated review. International Journal of Pharmaceutical Investigation 2012;2:2. https://doi.org/10.4103/2230-973x.96920.

[2] Heng PWS. Controlled release drug delivery systems. Pharmaceutical Development and Technology 2018;23:833. https://doi.org/10.1080/10837450.2018.1534376.

[3] Adepu S, Ramakrishna S. Controlled Drug Delivery Systems: Current Status and Future Directions. Molecules 2021;26:5905. https://doi.org/10.3390/molecules26195905.

[4] Haj-Ahmad R, Rasekh M, Nazari K, Li Y, Fu Y, Li B, Zhang Q, Xia Z, Liu H, Gu T, Wang G, Kucuk I, Khan H, Arshad M, Li X, Ahmad Z. EHDA Spraying: A Multi-Material Nano-Engineering Route. Current Pharmaceutical Design 2015;21:3239–47. https://doi.org/10.2174/1381612821666150531171506.

[5] Munir MM, Suryamas AB, Iskandar F, Okuyama K. Scaling law on particle-to-fiber formation during electrospinning. Polymer 2009;50:4935–43. https://doi.org/10.1016/j.polymer.2009.08.011.

[6] Yurteri CU, Hartman RPA, Marijnissen JCM. Producing Pharmaceutical particles via Electrospraying with an emphasis on nano and nano structured particles - A review. KONA Powder and Particle Journal 2010;28:91–115. https://doi.org/10.14356/kona.2010010.

[7] Kusumah FH, Sriyanti I, Edikresnha D, Munir MM, Khairurrijal. Simply electrospun gelatin/cellulose acetate nanofibers and their physico-Chemical characteristics. Materials Science Forum 2017;880:95–8. https://doi.org/10.4028/www.scientific.net/MSF.880.95.

[8] Andrady AL. Science and Technology of Polymer Nanofibers. Canada: John Wiley & Sons, Inc.; 2007. https://doi.org/10.1002/9780470229842.

[9] Ramakrishna S, Fujihara K, Teo WE, Lim TC, Ma Z. An introduction to electrospinning and nanofibers. Singapore: World Scientific Publishing Co. Pte. Ltd.; 2005. https://doi.org/10.1142/5894.

[10] Sridhar R, Ramakrishna S. Electrosprayed nanoparticles for drug delivery and pharmaceutical applications. Biomatter 2013;3:1–12. https://doi.org/10.4161/biom.24281.

[11] Franco P, De Marco I. The use of poly(N-vinyl pyrrolidone) in the delivery of drugs: A review. Polymers 2020;12:18–21. https://doi.org/10.3390/POLYM12051114.

[12] Chen Y, Wang J, Rao Z, Hu J, Wang Q, Sun Y, Lei X, Zhao J, Zeng K, Xu Z, Ming J. Study on the stability and oral bioavailability of curcumin loaded (-)-epigallocatechin-3-gallate/poly(N-vinylpyrrolidone) nanoparticles based on hydrogen bonding-driven self-assembly. Food Chemistry 2022;378:132091. https://doi.org/10.1016/j.foodchem.2022.132091.

[13] Alfatama M, Shahzad Y, Choukaife H. Recent advances of electrospray technique for multiparticulate preparation: Drug delivery applications. Advances in Colloid and Interface Science 2024;325:103098.

https://doi.org/10.1016/j.cis.2024.103098.
[14] Bock N, Woodruff MA, Hutmacher DW, Dargaville TR. Electrospraying, a reproducible method for production of polymeric microspheres for biomedical applications. Polymers 2011;3:131–49. https://doi.org/10.3390/polym3010131.
[15] Xu Y, Skotak M, Hanna M. Electrospray encapsulation of water-soluble protein with polylactide. I. Effects of formulations and process on morphology and particle size. Journal of Microencapsulation 2006;23:69–78. https://doi.org/10.1080/02652040500435048.
[16] Nguyen DN, Clasen C, Van den Mooter G. Pharmaceutical Applications of Electrospraying. Journal of Pharmaceutical Sciences 2016;105:2601–20. https://doi.org/10.1016/j.xphs.2016.04.024.
[17] Chow HHS, Hakim IA. Pharmacokinetic and chemoprevention studies on tea in humans. Pharmacological Research 2011;64:105–12. https://doi.org/10.1016/j.phrs.2011.05.007.
[18] Ma C, Xie Y, Huang X, Zhang L, Julian McClements D, Zou L, Liu W. Encapsulation of (-)-epigallocatechin gallate (EGCG) within phospholipid-based nanovesicles using W/O emulsion-transfer methods: Masking bitterness and delaying release of EGCG. Food Chemistry 2024;437:137913. https://doi.org/10.1016/j.foodchem.2023.137913.
[19] Kerio LC, Wachira FN, Wanyoko JK, Rotich MK. Total polyphenols, catechin profiles and antioxidant activity of tea products from purple leaf coloured tea cultivars. Food Chemistry 2013;136:1405–13. https://doi.org/10.1016/j.foodchem.2012.09.066.
[20] Parvez S, Wani IA. Exploring the antioxidant realm of green tea: From extraction to fortification. EFood 2024;5:1–18. https://doi.org/10.1002/efd2.172.
[21] Purwanto DA, Agustin BD, Ekowati J. A study of the stability of antioxidant activity of green tea extract powder with vitamin C. Pharmacy Education 2023;23:159–63. https://doi.org/10.46542/pe.2023.234.159163.
[22] Suzuki T, Kumazoe M, Kim Y, Yamashita S, Nakahara K, Tsukamoto S, Sasaki M, Hagihara T, Tsurudome Y, Huang Y, Maeda-Yamamoto M, Shinoda Y, Yamaguchi W, Yamada K, Tachibana H. Green tea extract containing a highly absorbent catechin prevents diet-induced lipid metabolism disorder. Scientific Reports 2013;3:1–7. https://doi.org/10.1038/srep02749.
[23] Namal Senanayake SPJ. Green tea extract: Chemistry, antioxidant properties and food applications - A review. Journal of Functional Foods 2013;5:1529–41. https://doi.org/10.1016/j.jff.2013.08.011.
[24] Chen IJ, Liu CY, Chiu JP, Hsu CH. Therapeutic effect of high-dose green tea extract on weight reduction: A randomized, double-blind, placebo-controlled clinical trial. Clinical Nutrition 2016;35:592–9. https://doi.org/10.1016/j.clnu.2015.05.003.
[25] Kamaruddin, Edikresnha D, Sriyanti I, Munir MM, Khairurrijal. Synthesis of Polyvinylpyrrolidone (PVP)-Green Tea Extract Composite Nanostructures using Electrohydrodynamic Spraying Technique. IOP Conference Series: Materials Science and Engineering 2017;202:012043. https://doi.org/10.1088/1757-899X/202/1/012043.
[26] Kamaruddin, Sriyanti I, Edikresnha D, Munir MM, Khairurrijal K. Electrosprayed Polyvinylpyrrolidone (PVP) Submicron Particles Loaded by Green Tea Extracts. IOP Conference Series: Materials Science and Engineering 2018;367:012036. https://doi.org/10.1088/1757-899X/367/1/012036.
[27] Sriyanti I, Edikresnha D, Rahma A, Munir MM, Rachmawati H, Khairurrijal K. Correlation between Structures and Antioxidant Activities of Polyvinylpyrrolidone/ Garcinia mangostana L. Extract Composite Nanofiber Mats Prepared Using Electrospinning. Journal of Nanomaterials 2017;2017:1–10. https://doi.org/10.1155/2017/9687896.
[28] Sriyanti I, Edikresnha D, Rahma A, Munir MM, Rachmawati H, Khairurrijal K. Mangosteen pericarp extract embedded in electrospun PVP nanofiber mats: Physicochemical properties and release mechanism of α-mangostin. International Journal of Nanomedicine 2018;13:4927–41. https://doi.org/10.2147/IJN.S167670.
[29] Idjan MKNA, Fatmawati, Almafie MR, Dani R, Subandrate, Fudholi A, Sriyanti I. Physicochemical properties and antioxidant activity of PVP/CA membranes nanofiber loaded Arcangelisia flava L. Merr. stem extract using electrospinning technique. Next Materials 2025;8:100839. https://doi.org/10.1016/j.nxmate.2025.100839.
[30] Antolovich M, Prenzler PD, Patsalides E, McDonald S, Robards K. Methods for testing antioxidant activity. Analyst 2002;127:183–98. https://doi.org/10.1039/b009171p.
[31] Pusporini P, Edikresnha D, Sriyanti I, Suciati T, Munir MM, Khairurrijal K. Electrospun polyvinylpyrrolidone (PVP)/green tea extract composite nanofiber mats and their antioxidant activities. Materials Research Express 2018;5:1–9. https://doi.org/10.1088/2053-1591/aac1e6.
[32] Zhang D, La Zara D, Quayle MJ, Petersson G, Van Ommen JR, Folestad S. Nanoengineering of Crystal and Amorphous Surfaces of Pharmaceutical Particles for Biomedical Applications. ACS Applied Bio Materials 2019;2:1518–30. https://doi.org/10.1021/acsabm.8b00805.

[33] Sun CC, Davé RN. Crystal and Particle Engineering – An Indispensable Tool for Developing and Manufacturing Quality Pharmaceutical Products. Pharmaceutical Research 2022;39:3041–5. https://doi.org/10.1007/s11095-022-03449-x.
[34] Vehring R. Pharmaceutical particle engineering via spray drying. Pharmaceutical Research 2008;25:999–1022. https://doi.org/10.1007/s11095-007-9475-1.
[35] Fromen CA, Shen TW, Larus AE, Mack P, Maynor BW, Luft JC, Desimone JM. Synthesis and characterization of monodisperse uniformly shaped respirable aerosols. AIChE Journal 2013;59:3184–94. https://doi.org/10.1002/aic.14157.
[36] Widiyandari H, Hogan CJ, Yun KM, Iskandar F, Biswas P, Okuyama K. Production of Narrow-Size-Distribution Polymer-Pigment-Nanoparticle Composites via Electrohydrodynamic Atomization. Macromolecular Materials and Engineering 2007;292:495–502. https://doi.org/10.1002/mame.200600427.
[37] Zhang S, Kawakami K. One-step preparation of chitosan solid nanoparticles by electrospray deposition. International Journal of Pharmaceutics 2010;397:211–7. https://doi.org/10.1016/j.ijpharm.2010.07.007.
[38] Wang XX, Ju XJ, Sun SX, Xie R, Wang W, Liu Z, Chu LY. Monodisperse erythrocyte-sized and acid-soluble chitosan microspheres prepared via electrospraying. RSC Advances 2015;5:34243–50. https://doi.org/10.1039/c5ra04726a.
[39] Rahma A, Munir MM, Khairurrijal, Prasetyo A, Suendo V, Rachmawati H. Intermolecular Interactions and the Release Pattern of Electrospun Curcumin-Polyvinyl(pyrrolidone) Fiber. Biological and Pharmaceutical Bulletin 2016;39:163–73. https://doi.org/10.1248/bpb.b15-00391.
[40] Rezeki YA, Hapidin DA, Rachmawati H, Munir MM, Khairurrijal K. Formation of electrosprayed composite nanoparticles from polyvinylpyrrolidone/mangosteen pericarp extract. Advanced Powder Technology 2020;31:1811–24. https://doi.org/10.1016/j.apt.2020.02.016.
[41] Xie J, Jiang J, Davoodi P, Srinivasan MP, Wang C-H. Electrohydrodynamic atomization: A two-decade effort to produce and process micro-/nanoparticulate materials. Chemical Engineering Science 2015;125:32–57. https://doi.org/10.1016/j.ces.2014.08.061.
[42] Wang J, Xu H, Huo Y, Wang Y, Dong M. Progress of electrospray and electrospinning in energy applications. Nanotechnology 2020;31:1–22. https://doi.org/10.1088/1361-6528/ab52bb.
[43] Hogan CJ, Yun KM, Chen DR, Lenggoro IW, Biswas P, Okuyama K. Controlled size polymer particle production via electrohydrodynamic atomization. Colloids and Surfaces A: Physicochemical and Engineering Aspects 2007;311:67–76. https://doi.org/10.1016/j.colsurfa.2007.05.072.
[44] Reksamunandar RP, Edikresnha D, Munir MM, Damayanti S, Khairurrijal. Encapsulation of β-carotene in poly(vinylpyrrolidone) (PVP) by Electrospinning Technique. Procedia Engineering, vol. 170, Procedia Engineering; 2017, p. 19–23. https://doi.org/10.1016/j.proeng.2017.03.004.
[45] Senthilkumar SR, Sivakumar T. Green tea (Camellia sinensis) mediated synthesis of zinc oxide (ZnO) nanoparticles and studies on their antimicrobial activities. International Journal of Pharmacy and Pharmaceutical Sciences 2014;6:461–5.
[46] Manea A-M, Vasile BS, Meghea A. Antioxidant and antimicrobial activities of green tea extract loaded into nanostructured lipid carriers. Comptes Rendus Chimie 2013;17:331–41. https://doi.org/10.1016/j.crci.2013.07.015.
[47] Pool H, Quintanar D, Figueroa JDD, Marinho Mano C, Bechara JEH, Godínez LA, Mendoza S. Antioxidant effects of quercetin and catechin encapsulated into PLGA nanoparticles. Journal of Nanomaterials 2012;2012:12 Pages. https://doi.org/10.1155/2012/145380.